Acta Cryst. (1966). **20**, 283

The Vaterite-Type ABO_3 Rare-Earth Borates*

BY W. F. BRADLEY
Dept. of Chemical Engineering, University of Texas, Austin, Texas, U.S.A.

D. L. GRAF
Illinois State Geological Survey, Urbana, Illinois, U.S.A.

AND R. S. ROTH
National Bureau of Standards, Washington, D.C., U.S.A.

(*Received* 27 *October* 1964 *and in revised form* 4 *June* 1965)

Approximate models are proposed for the room temperature and the high temperature modifications of the vaterite-type rare earth borates. A low temperature model based on three-membered rings of borate tetrahedra is found to be reconcilable with the X-ray powder diffraction data, the optical properties, and the infrared absorption character. A high-temperature model containing triangular borate ions is relatable to the $CaCO_3$ vaterite modification.

Introduction

A survey of polymorphism of ABO_3 type rare earth borates by Levin, Roth & Martin (1961) established that borates of the rare earths from lutecium to samarium exhibited one polymorph recognizably related to vaterite ($CaCO_3$), and that each room-temperature product was an inversion from a high-temperature form dimensionally much more closely related to vaterite, but subject to excessive fragmentation on cooling. The room-temperature forms were found to be optically positive with low birefringence. X-ray diffraction data were limited to the powder method.

Major features of the vaterite and the rare earth vaterite powder diffraction diagrams are all indexable on the basis of hexagonal cells of two formula-weight content.

A description by McConnell (1960) of a naturally occurring vaterite took account of the observation by Bunn (1945) that high positive birefringence demands that the CO_3 groups stand vertical, and that any hexagonal or trigonal unit cell must contain $6CaCO_3$. On preferred-orientation electron diffraction diagrams, McConnell observed two features which required the larger cell, and adopted it for indexing, noting that an alternation of orientation of successive vertical triads was required.

Powder data for all compositions fix cation positions as 0, 0, 0 and 0, 0, $\frac{1}{2}$ in the two-formula subcell. Bartram & Felten (1961) and Newnham, Redman & Santoro (1963), working on low-temperature rare earth borates, and Kamhi (1963), on vaterite, have each evaluated anion parameters which represented averaged positions within this subcell. Newnham *et al.* further noted that ordered arrays in the six-formula cell could exist, and cited one arrangement in the space group $P6_3/mcm$ which provides six vertical BO_3 groups.

Infrared absorption analyses by Weir & Lippincott (1961) and Weir & Schroeder (1964) disclosed that boron in the low temperature rare earth vaterite-type borates is in fourfold coordination. The B–O stretching frequencies are about 250 cm^{-1} lower for the vaterite-type borates than for the ν_3 mode in the calcite isotype, $LuBO_3$, or the aragonite isotype, $LaBO_3$.

It is the objective of this analysis to propose models for the low and high temperature borates which are consistent with the optical and absorption properties, and with the X-ray powder diffraction diagrams.

Data for $YbBO_3$ are taken as typical for the group. For the low temperature form $a_0=6{\cdot}46$, $c_0=8{\cdot}74$ Å, $Z=6$, and $c/a=1{\cdot}341$; for the high temperature form, $a_0=6{\cdot}99$, $c_0=8{\cdot}34$ Å, $Z=6$, and $c/a=1{\cdot}193$. For vaterite, $a_0=7{\cdot}135$, $c_0=8{\cdot}524$ Å, and $c/a=1{\cdot}195$.

The low temperature form

Integrated relative intensities were collected by diffractometer technique from the $YbBO_3$ powder prepared by Levin, Roth & Martin (1961). The data, which are summarized in Table 1, include five lines with intensities only 5% to 10% above background and six even weaker or doubtful features which can be indexed only in the six-formula cell. Indexing was facilitated by the tabular morphology of the grains. Powder lines are of graded sharpness, ranging from sharp for reflections with $l=0$ to increasingly broad with increasing l indices. At large diffraction angles, α_1–α_2 resolution becomes apparent for reflections with $l=0$.

Relationships between the true hexagonal cell with $a_0=6{\cdot}46$ Å and the two-formula subcell with $a'=a_0/\sqrt{3}$ are best defined if subcell origins are shifted to $\frac{1}{2}$, $\frac{1}{2}$.

* This work was done in part at the Computation Center of the Massachusetts Institute of Technology, during the tenure of a Research Fellowship extended to D. L. Graf by the Committee on Experimental Geology and Geophysics of Harvard University.

Table 1. *Powder diffraction data for* $YbBO_3$

Probable space group $P\bar{6}c2$: $a_0=6{\cdot}46$, $c_0=8{\cdot}74$Å, $Z=6$

Filtered Cu radiation

d_{calc}(Å)	d_{obs}(Å)	$hk{\cdot}l$	Integrated diffractometer count*†	Normalized F_{obs}	F_{calc} . exp $\{-0{\cdot}2\,(\sin\theta/\lambda)^2\}$ I	II
5·60		$1\bar{1}{\cdot}0$	—		12	16
4·37	4·36	00·2	1240	334	325	330
3·45	3·44	$1\bar{1}{\cdot}2$	(7)	13	21	26
3·23	3·23	11·0	3060	417	312	317
3·03	3·02	11·1	90	56	33	30
2·80	2·80	$2\bar{2}{\cdot}0$	(<4)	<17	16	11
2·60	2·60	11·2	3114	378	354	356
2·356	2·35	$2\bar{2}{\cdot}2$	(<4)	<15	20	17
2·185	2·18	00·4	205	290	309	315
2·163	2·16	11·3	20	33	44	47
2·114	2·11	21·0	(<4)	<16	14	18
2·055	2·06	21·1	(8)	17	29	26
2·035	2·04	$1\bar{1}{\cdot}4$	(7)	23	23	27
1·903	1·90	21·2	(<4)	<13	12	16
1·865	1·866	$3\bar{3}{\cdot}0$	772	393	355	356
1·809	1·810	11·4	1020	331	318	324
1·721		$2\bar{2}{\cdot}4$	not resolved		30	30
1·715	1·716	$3\bar{3}{\cdot}2$	779	309	295	303
1·712		21·3			4	5
1·615	1·616	22·0	235	259	266	269
1·588	1·587	22·1	16	47	35	26
1·552		31·0	—		9	9
1·538	1·538	11·5	(4)	24	25	24
1·527		31·1	—		5	13
1·520		21·4	—		10	13
1·515	1·515	22·2	462	277	285	297
1·457	1·457	00·6	36	200	235	237
1·418	1·419	$3\bar{3}{\cdot}4$	254	223	241	250
1·412		22·3				17
1·400		$4\bar{4}{\cdot}0$				11
1·369	1·37	31·3	(<4)	<19	22	19
1·332		$4\bar{4}{\cdot}2$	not resolved		17	28
1·328	1·328	11·6	270	248	271	280
1·299	1·299	22·4	301	269	264	265
1·292		$2\bar{2}{\cdot}6$			11	5
1·283	1·28	32·0	(4)	31	14	11
1·276		32·1			9	6
1·265	1·26	31·4	(<4)	<22	17	18
1·232		32·2			8	8
1·221	1·222	41·0	183	224	243	260
1·209		41·1			14	9
1·178		$4\bar{4}{\cdot}4$	not resolved		24	34
1·176	1·177	41·2	385	269	234	236
1·166		11·7	?		20	20
1·162		31·5			16	11
1·147	1·148	$3\bar{3}{\cdot}6$	134	202	230	238

All succeeding combinations for which $h-k\neq 3n$ have calculated intensities less than 1 % of background

1·092	1·093	00·8	46	300	283	291
1·082	1·083	22·6	284*	220	235	249
1·076	1·078	33·0		263	234	236
1·066	1·067	41·4	352	232	242	257
1·045	1·047	33·2	207	242	232	245
1·035	1·036	11·8	144	210	203	214
0·966	0·967	33·4	110	190	194	201
0·943	0·94	$3\bar{3}{\cdot}8$	494*		232	236
0·936		41·6			205	207
0·9325	0·9326	$6\bar{6}{\cdot}0$	about	200	213	217

* Two high angle complex features marked with an asterisk had superimposed on them enough α_1/α_2 resolution for the prism member to permit that it be estimated separately.

† Five entries for which counts were between 5 and 10 % of background are enclosed in parentheses and six lesser counts are similarly indicated. The count for 22·1 was 20 % above background.

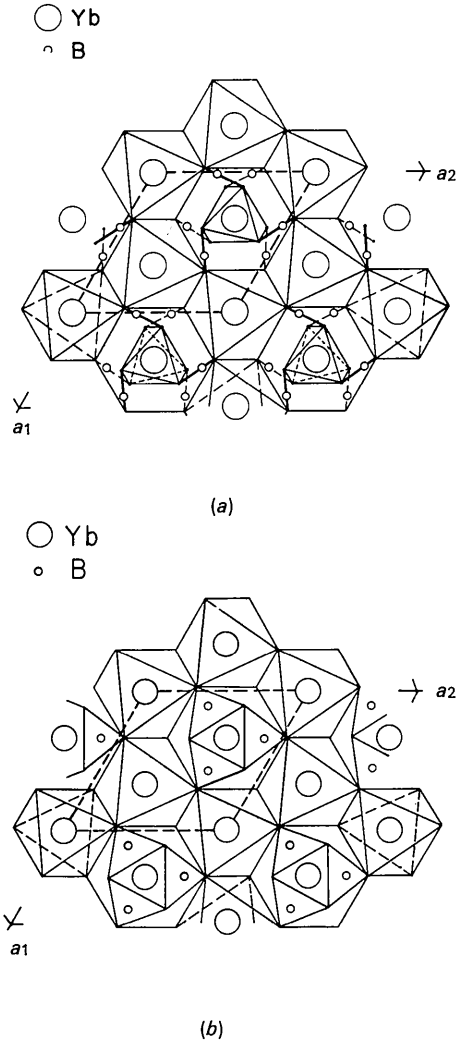

Fig. 1. *c*-Axis projection of edge-sharing nets of YbO_6 octahedra as coordinated about two of the rare earth ions in one half of a low temperature form unit cell. In (*a*), the profiles of triangular borate ions above this net are indicated by heavy lines to the corners which they share with octahedra, and the positions of ions below the net by light lines. In (*b*), only the articulation of the three-membered ring of tetrahedra above the net is indicated. Each arrangement surrounds the third rare earth ion with 6 O(1) and 6 O(2) oxygen atoms. In either model the structure is completed by the operation of the mirror planes at $z=\frac{1}{4}$ and $\frac{3}{4}$. O(2) oxygen atoms and boron lie in these planes. a_1 and a_2 for $YbBO_3$ are 6·46 Å.

The rare earth cations in special positions are then located at $\frac{1}{2}$, $\frac{1}{2}$, 0 and $\frac{1}{2}$, $\frac{1}{2}$, $\frac{1}{2}$, and each has a coordination environment within its own subcell.

The contributions of the Yb atoms in special positions so dominate the intensities of reflections with $h-k=3n$ and $l=2n$ that any placement of anions would afford adequate agreement with a powder diagram, but the eleven weak reflections with $h-k\neq 3n$ require that the placement of anions in one subcell must differ from that in the other two. Single layers of composition $3YbBO_3$ which meet this requirement are illustrated in Fig. 1. In each, oxygen atoms in twelvefold positions, designated O(1), are symmetrically displaced from the averaged subcell positions derived by Newnham, Redman & Santoro (1963) to provide nets of edge-sharing octahedra about Yb in two subcells. Extinction criteria and this model are consistent with the space group $P\bar{6}c2$. In $P\bar{6}c2$, these oxygen atoms are in general positions with $x=\frac{1}{3}$, $y\simeq 0{\cdot}05$ and $z=0{\cdot}117$. The structure is completed by addition of boron and oxygen atoms, designated O(2), in sixfold positions on the mirror planes at $z=\frac{1}{4}$ and $z=\frac{3}{4}$. These mirror-plane oxygen atoms together with the general position set afford twelvefold coordination about the Yb in the third subcell.

Ordered arrangements in this model can lead either to a triangular boron coordination, analogous with vaterite, or to a three-membered ring of 4-coordinated boron tetrahedra. The two alternatives are illustrated in Fig. 1(*a*) and (*b*) respectively. In Fig. 1(*a*), borate triangles with B–O bond lengths of 1·34 Å are indicated in profile, and in Fig. 1(*b*) four B–O bond lengths of 1·46 Å are assumed.

Calculated amplitudes for the triangular model, 'calculated I', and for the tetrahedral model, 'calculated II', are compared with observed *F*'s, normalized to agreement for major terms, in Table 1. Each set is a best agreement selected from several slightly varied parameter assumptions. For either set the discrepancy indices for major terms are of the order of 0·1. Three entries for which $h-k=3n$ with l odd, and eleven entries for which $h-k\neq 3n$ derive their total amplitudes from anion contributions. Discrepancy indices for these fourteen reflections are respectively 0·25 and 0·34, but both represent comparisons between two poorly established quantities. The normalized F_{obs} values for these weak reflections, based on intensities from 10% to less than 5% above background, are necessarily

Table 2. *Choice between triangular and tetrahedral arrangement*

	Triangular model	Tetrahedral model	Observed
Major term discrepancy index	0·1	0·1	
Discrepancy index for anion-only reflections	0·25	0·34	
Estimated B–O stretching frequency*	1250	1000	800–1100
Optic sign	+		+
Probable birefringence†	near 0·05	0·001 to 0·01	0·007–0·014

* From Weir & Schroeder (1964). They also cite absence of sufficiently large isotropic shift in any frequency which could be attributed to an out-of-plane bending mode for a triangular anion.

† Predicted by comparison with $InBO_3$ and R_2O_3 rhombohedral oxides respectively.

subject to large uncertainty, and calculated amplitude sums for low angle reflections are strongly dependent upon arbitrary selection of atomic, ionic, or hybrid scattering factors. The sums cited are for atomic factors. The magnitudes of these discrepancy factors establish that both boron and oxygen are differently placed in different subcells. They indicate that either model is approximately reconciled with the powder data, but do not afford a clear choice between them. Either level of agreement is superior to that possible in the model of Newnham *et al.* (1963), in which only boron can contribute to amplitudes when $h-k \neq 3n$.

The tabular habit, with consequent uncertain relation of intensities of prism reflections to those with non-zero l index, and the cited data limitations preclude meaningful additional refinement. A further observation, that greatest excesses of observed amplitudes over calculated involve directions near [110], suggests that the tabular crystallites may actually be dendritic.

A summary of information pertinent to choice between the triangular and tetrahedral arrangements is collected in Table 2. The strict requirements of the optical character and absorption spectral criteria demand the choice of the tetrahedral. Atom parameters for this model are listed in Table 3. The ranges in which other interatomic distances fall when 1·46 Å B–O bond lengths are assumed and O(1) parameters near that adopted for the $YbBO_3$ composition are applied to the other rare earth compositions are summarized in Table 4. In all cases octahedrally coordinated cation–oxygen distances approximate known radius sums for octahedral coordination, and cation–oxygen distances in the 12-coordination polyhedra are about $\frac{1}{6}$ longer.

For the tetrahedral model electrostatic bond strength summations about O(1) are $\frac{1}{2}$ each to Yb(2) and Yb(3), $\frac{1}{4}$ to Yb(1) and $\frac{3}{4}$ to B, and about O(2) are $\frac{1}{4}$ each to two Yb(1) and $\frac{3}{4}$ each to two B.

The high-low inversion

The limited data available in the powder diffraction diagram of high temperature $YbBO_3$ taken at 1100 °C (Levin, Roth & Martin, 1961) is cited in Table 5.

The inversion to the low temperature form, from an originally synthesized high temperature modification, involves shrinkage in the **a** directions and expansion along **c**. For the $YbBO_3$, the a axes shorten from 6·99 to 6·46 Å and the c axis expands from 8·34 to 8·74 Å. Nets of edge-sharing octahedra in layer structures generally exhibit layer thicknesses near 2·1 or 2·2 Å, as is observed for the low temperature form. If the boron and oxygen ions are to be accommodated in the remaining space in the high temperature form they must be present as borate triangles inclined to the c axis. A similar conclusion can be inferred from dimensions of the $CaCO_3$ analogue. Its c-axis length of 8·52 Å is interpreted as accommodating Ca octahedra and vertically disposed CO_3 ions, *i.e.* an axis nearly 0·2 Å lon-

Table 3. *Atom parameters in* $P\bar{6}c2$ *for* $YbBO_3$ *(low temperature form)*

12	O(1)	in	12(*l*)	x, y, z; *etc.* with $x=\frac{1}{3}$, $y=0{\cdot}047$, $z=0{\cdot}117$
6	O(2)	in	6(*k*)	$x, y, \frac{1}{4}$; *etc.* with $x=\frac{1}{3}$, $y=0{\cdot}44$
6	B	in	6(*k*)	with $x=\frac{1}{3}$, $y=-0{\cdot}10$
2Yb(1)		in	2(*c*)	$\frac{1}{3}, \frac{2}{3}, 0$; $\frac{1}{3}, \frac{2}{3}, \frac{1}{2}$
2Yb(2)		in	2(*e*)	$\frac{2}{3}, \frac{1}{3}, 0$; $\frac{2}{3}, \frac{1}{3}, \frac{1}{2}$
2Yb(3)		in	2(*a*)	0, 0, 0; 0, 0, $\frac{1}{2}$

Table 4. *Internally consistent interatomic distances in the low temperature vaterite-type rare earth borate compositions* (Lu *to* Sm) *based on* 1·46 Å *for* B–O *in tetrahedra*

	When $y_{O(1)}=0{\cdot}04$	When $y_{O(1)}=0{\cdot}05$
Lu(1)–O(1) to Sm(1)–O(1)	2·62 – 2·71	2·68 – 2·77
Lu(1)–O(2) to Sm(1)–O(2)	2·63 – 2·71	
Lu(2), (3)–O(1) to Sm(2), (3)–O(1)	2·28 – 2·37	2·26 – 2·34
O(1)–O(1) (shared edge)		
in Lu	2·61	2·53
in Sm	2·74	2·66
O(1)–O(1) (out of plane)		
in Lu	3·13	3·21
in Sm	3·30	3·36
O(1)–O(1) (in plane)		
in Lu	3·51	3·47
in Sm	3·64	3·60
O(2)–O(2) (shared face)		
in Lu	2·54	
in Sm	2·63	

Table 5. *Powder diffraction diagram for* $YbBO_3$ *taken at* 1100 °C

Probable space group $P6_322$: $a_0=6{\cdot}99$, $c_0=8{\cdot}34$ Å
Filtered Cu radiation

d_{obs}(Å)	$hk{\cdot}l$	Relative intensity
4·16	00·2	5
3·49	11·0	10
3·22	11·1	$\frac{1}{2}$
3·04	20·0	$<\frac{1}{2}$
2·87	20·1	$<\frac{1}{2}$
2·67	11·2	10
2·44	20·2	tr
2·28	21·0	tr
2·08	00·4	1
2·05	20·3	tr
2·015	30·0	2
1·815	30·2	2
1·789	11·4	2
1·745	22·0	1
1·71	22·1	tr
1·605	22·2	$2\frac{1}{2}$
1·51	40·0	$<\frac{1}{2}$
1·450	30·4	$1\frac{1}{2}$
1·39	00·6	tr
1·341	22·4	1
1·321	41·0	$\frac{1}{2}$
1·292	11·6	1
1·260	41·2	1

ger accommodates anions of 0·1 Å smaller mutual O–O contacts.

A shared-edge arrangement of Yb octahedra, condensed with tilted triangular anions, can be described in the space group $P6_322$. This space group permits contributions by the anion to the amplitude of both the classes *hhl* with *l* odd and *hh̄l* with *l* odd. Two powder lines of each class are observed. Fig. 2 depicts one layer of the expanded octahedral net with the two sets of three tilted triangular borate ions respectively above and below the octahedra. Only one (dashed) of the lower set is indicated. In $P6_322$ the Yb are located at $z=\frac{1}{4}$ and the structure is completed by the twofold operators on the *a* axes at $z=0$ and $\frac{1}{2}$. The net which is foreshortened by edge sharing affords octahedral environment to the Yb in positions 0, 0, $\frac{1}{4}$ and 0, 0, $\frac{3}{4}$. The columns of polyhedra about Yb at $\frac{1}{3}$, $\frac{2}{3}$ and $\frac{2}{3}$, $\frac{1}{3}$ are alternately large and small twelvefold environments related to each other by the twofold axes. In Fig. 2 the oxygen atoms in twelvefold equivalent positions are arbitrarily located at $x=0{\cdot}32$, $y=0{\cdot}07$. This provides room for borate triangles with B–O bond lengths near 1·35 Å and Yb–O distances of 2·26 Å in the octahedron about 0, 0, $\frac{1}{4}$. In the polyhedra of the 12-coordinated Yb one has six Yb–O distances near 2·4 and six near 2·9 Å; the other has twelve near 2·9 Å.

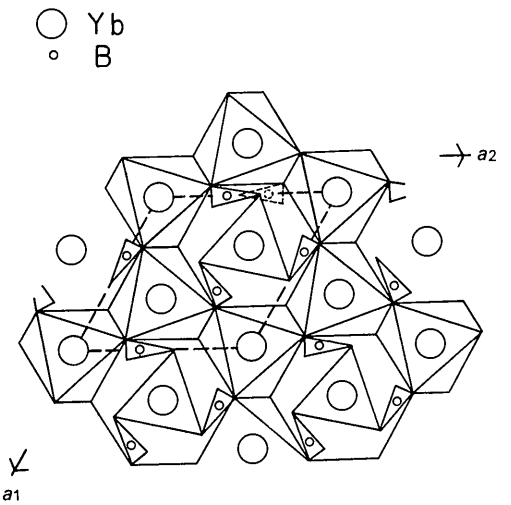

Fig. 2. *c*-Axis projection of a stretched net of edge-sharing octahedra like the Fig. 1 arrangements, but affording room for successive nets to be articulated by tilted triangular borate ions. The structure is completed by twofold rotation about *a* axes at $z=0$ and $\frac{1}{2}$. O(2) oxygen atoms and boron lie on these axes. a_1 and a_2 are 6·99 Å.

Although the arrangement of Fig. 2 must be taken as highly speculative, it permits reasonable inferences. The oxygen atoms in sixfold positions in either structure move furthest in the inversion. For example, the oxygen at $x=0{\cdot}43$, $y=0{\cdot}43$ in the high temperature form moves to $x=\frac{1}{3}$, $y=0{\cdot}44$ in the low temperature form. It may be presumed to have the greatest individual thermal amplitude. If, with declining thermal motion, O(1) oxygen are to seek equal Yb–O bond lengths to their three Yb neighbors, the triangular borate ions must rotate to vertical, expanding the **c** direction, shrinking the lateral net, and permitting the condensation into three-membered rings of borate tetrahedra in one or the other of the low temperature subcells.

With respect to any one layer in this high temperature model, a vertical set of triangles locate twelvefold oxygen in one ordered choice from among the 36 alternatives of the disordered array adopted by Kamhi (1963) for $CaCO_3$ vaterite. The parameters $x=0{\cdot}32$, $y=0{\cdot}07$ of the O(2) oxygen (Fig. 2) become $x=0{\cdot}39$, $y=0{\cdot}78$ when referred to Kamhi's subcell. His solution (for $CaCO_3$) was $x=0{\cdot}38$, $y=0{\cdot}76$. The other six oxygen atoms are in an ordered sixfold choice with parameters approximating Kamhi's in magnitude, but opposite in sign.

The authors would like to thank Dr H. M. Ondik and Mr C. E. Weir for many informative discussions.

References

BARTRAM, S. F. & FELTEN, E. J. (1961). *Rare Earth Research Proc. 2nd Conf.* Sept. 24–27, 1961. Ed. J. F. Nachman and C. E. Lundin; Gordon and Breach Publishers (1962).
BUNN, C. W. (1945). *Chemical Crystallography*. Oxford.
KAMHI, S. R. (1963). *Acta Cryst.* **16**, 770.
LEVIN, E. M., ROTH, R. S. & MARTIN, J. B. (1961). *Amer. Min.* **46**, 1030.
MCCONNELL, J. D. C. (1960). *Miner. Mag.* **32**, 535.
NEWNHAM, R. E., REDMAN, M. J. & SANTORO, R. P. (1963). *J. Amer. Ceram. Soc.* **46**, 253.
WEIR, C. E. & LIPPINCOTT, E. R. (1961). *J. Res. Nat. Bur. Stands.* **65A**, 173.
WEIR, C. E. & SCHROEDER, R. A. (1964). *J. Res. Nat. Bur. Stands.* **68A**, 465.